Applied Physics Letters

Soluble alkali-metal carbon nanotube salts for n-type thermoelectric composites with improved stability

Cite as: Appl. Phys. Lett. **118**, 213901 (2021); https://doi.org/10.1063/5.0047338
Submitted: 12 February 2021 . Accepted: 04 May 2021 . Published Online: 25 May 2021

Bernhard Dörling, Xabier Rodríguez-Martínez, Ivan Álvarez-Corzo, J. Sebastian Reparaz, and Mariano Campoy-Quiles

Applied Physics Letters ARTICLE scitation.org/journal/apl

Soluble alkali-metal carbon nanotube salts for n-type thermoelectric composites with improved stability

Cite as: Appl. Phys. Lett. **118**, 213901 (2021); doi: 10.1063/5.0047338
Submitted: 12 February 2021 · Accepted: 4 May 2021 ·
Published Online: 25 May 2021

Bernhard Dörling, Xabier Rodríguez-Martínez, Ivan Álvarez-Corzo, J. Sebastian Reparaz, and Mariano Campoy-Quiles[a)]

AFFILIATIONS

Institute of Materials Science of Barcelona, ICMAB-CSIC, Campus UAB, 08193 Bellaterra, Spain

Note: This paper is part of the APL Special Collection on Organic and Hybrid Thermoelectrics.
[a)]**Author to whom correspondence should be addressed:** mcampoy@icmab.es

ABSTRACT

We present a method to dissolve carbon nanotubes that simultaneously allows to prepare n-doped films. These films are composed of thinner bundles of longer tubes when compared to films prepared using surfactants and sonication. Their negative Seebeck coefficient and high electrical conductivity make them good candidates for thermoelectric applications. We investigate their stability in air by aging them at elevated temperatures, showing stabilities over 500 h, which is further improved by the use of crown ethers. Finally, we demonstrate the usefulness of the prepared materials by fabricating an organic thermoelectric generator comprising 40 legs.

Carbon nanotubes (CNTs) are a promising thermoelectric material[1] due to their large electrical conductivity, and in the case of precisely doped semiconducting single-walled CNTs (SWCNTs), their potentially high Seebeck coefficient.[2,3] While there are many encouraging reports of p-type doped CNTs and other organic materials, n-type materials still lag behind,[4,5] particularly when considering their inferior stability.[6] Polyethyleneimine (PEI) has been used as an easy to process and effective n-type dopant for a long time.[7] Reports regarding its air-stability varied widely in the past, while nowadays it is accepted that some kind of barrier layer is required for prolonged air-stable operation.[8,9] Another more recent class of n-type dopant used for CNT thermoelectrics are crown-ether complexes of alkali metals. Doped mixtures of semiconducting and metallic tubes have shown good stability, which seemed to further improve with increasing CNT diameter.[5] However, somewhat disappointingly, the electrical conductivity of thin films of semiconducting SWCNTs with a diameter of less than 1.7 nm n-doped in this way was found to be unstable, degrading within minutes upon exposure to air,[6] which warrants further investigation.

In the same work, it was found that maximum doped electrical conductivity of CNT films correlates with a higher maximum power factor at optimum doping level.[6] This means that any (semiconducting) CNT raw material that is known to have an intrinsically high electrical conductivity could potentially also show a high power factor, if doped optimally.

Besides a high-quality raw material, and doping, there are other ways to further increase the electrical conductivity of CNTs. For example, decreasing the bundle-size in random carbon nanotube networks has been shown to increase the electrical conductivity in general,[10–12] and the thermoelectric power factor in particular.[6,13] Similarly, increased CNT length has been shown to result in an increased electrical conductivity.[14]

Here we report on a method that tries to combine several advantages into a unified approach. It allows to prepare n-doped films composed of smaller bundles of longer CNTs, when compared to other approaches.

The method joins two approaches: the n-type doping of buckypapers for thermoelectric applications using alkali metal-crown ether complexes as introduced by Nonoguchi *et al.*,[5] and the processing of CNTs from real solutions, again, using alkali metals,[15–17] or their crown ether complexes.[18–20] In the literature, the latter may be referred to as reduced carbon nanotubes,[21] CNT salts,[15] CNT polyelectrolytes,[16] or carbon nanotubides,[20] and interestingly, their thermoelectric properties have not been studied yet.

As raw material, we used enhanced direct injection pyrolytic synthesis (eDIPS) SWCNTs (Meijo Nano Carbon), which are comprised of comparatively long tubes (5 to 15 μm according to the manufacturer). All other materials were obtained from Sigma-Aldrich and used as received. The CNT salts were typically prepared by adding 50 mg (1.28 mmol) metallic potassium and 125 mg (0.975 mmol) naphthalene to 100 ml anhydrous Tetrahydrofuran (THF) in a nitrogen atmosphere, and stirred with a glass-coated stirring bar at room temperature for two hours. The resulting dark green naphthalenide solution contained no apparent solid residue. It was added to 10 mg (0.833 mmol of C) of eDIPS CNTs and further stirred for three days to one week. Then, the product was filtrated and washed with copious amounts of THF, to remove any traces of unreacted green napthalenide.

After drying in vacuum, the CNT salt was then dissolved in dimethyl sulfoxide (DMSO), for a final concentration of 0.1 mg ml^{-1} of CNTs. Some solutions additionally contained one of the crown ethers sketched in Fig. 1, namely, 18-crown-6 (18C6), benzo-18-crown-6 (B18C6), or dibenzo-18-crown-6 (DB18C6). They are known to sequester potassium ions and were added at a molar ratio of 1 crown ether per 20 carbon atoms. The solid was observed to slowly dissolve, forming a black liquid containing visible aggregates. As solutions were stirred for a further week, they progressively gelled as tubes debundled and dissolved. Solutions were diluted as needed and centrifuged at 6000 rpm for 1 h in sealed tubes outside the glovebox. Inside the glovebox, the solutions were stable for more than 18 months. Yet when directly exposed to air, tubes aggregate within minutes.

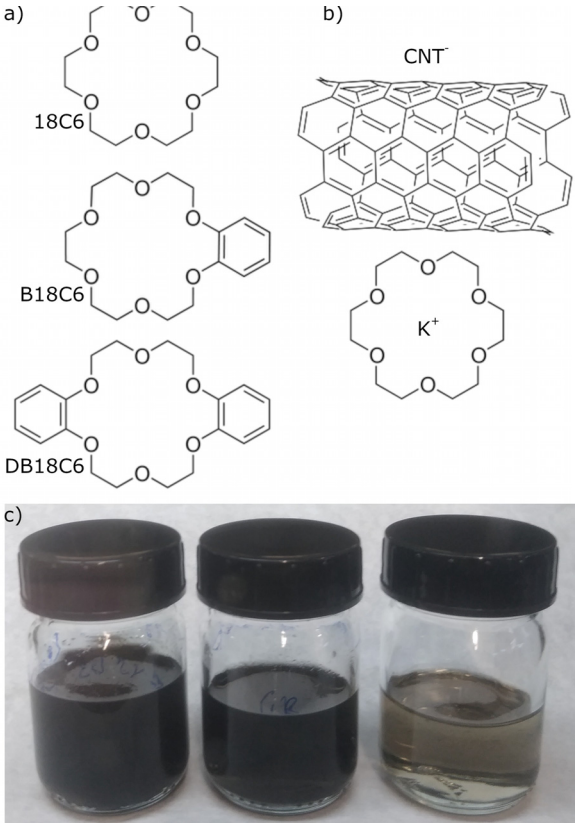

FIG. 1. (a) Structure of the crown ethers used in this study. (b) Sketch of one of several CNT salts used. (c) Photograph of 18 month old solutions containing DB18C6 before and after centrifugation, and after additional dilution from left to right, respectively.

Solutions in DMSO, like those shown in Fig. 1, were vacuum filtrated in the glovebox using 0.1 μm pore size polytetrafluoroethylene (PTFE) filters. The resulting films exhibit n-type characteristics, similar to earlier reports where films were doped in a post-processing step.[5] But because the tubes are not dispersed using damaging sonication, their length is not reduced, which is particularly beneficial for raw material that is composed of long tubes.[22–25] Additionally, tubes can be completely individualized in these real solutions. Deposited films show smaller bundle size, compared to films deposited from surfactant dispersions,[17,25] or even superacid solutions.[26]

This is clearly visible in the SEM images in Fig. 2, which compare the CNT salt to tubes dispersed in water, using sonication and sodium dodecylbenzenesulfonate (SDBS) as surfactant. To determine the film thickness, samples were mechanically delaminated from the PTFE filter and transferred to cleaned glass microscope slides. Transferring entire films of eDIPS CNTs can be accomplished rather easily, compared to other raw materials composed of shorter tubes, which result in more powdery films. Film thickness was measured using a Profilometer P16+ from KLA Tencor and ranged from about 300 to 900 nm.

Using a custom built setup, electrical conductivity σ and Seebeck coefficient S were measured on the same, approximately 3×1 cm^2 sized samples, which were contacted at the four corners by silver paint

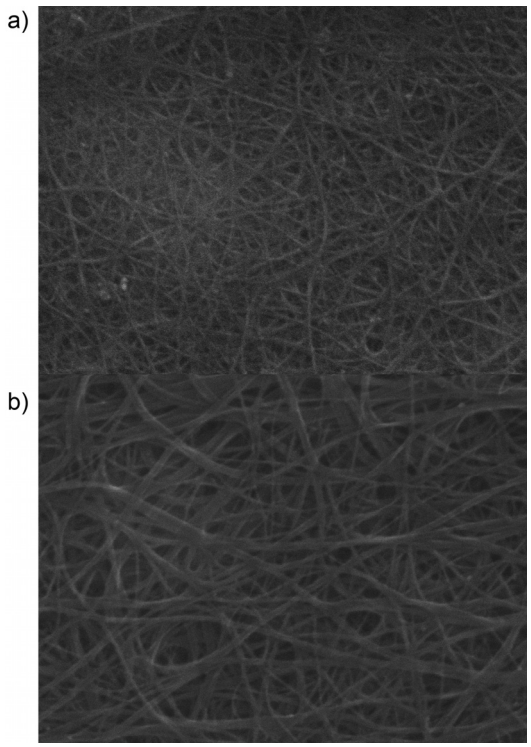

FIG. 2. SEM images of films (a) prepared from a CNT salt (K), and (b) of CNTs dispersed using SDBS.

and type T thermocouple probes.[27,28] σ was measured using the van der Pauw method,[29] using the copper leads of the thermocouples. The average Seebeck coefficient between 310 and 350 K was measured by heating up one side of the sample. The temperature gradient between the two sides was slowly ramped from 0 to 40 K and back at a speed of about 2 K/min. The temperature at each corner was measured with the individual thermocouples, while the Seebeck voltage across the sample was recorded using pairs of copper leads. Data were acquired with a Keithley 2400 SourceMeter. S was extracted from a straight line fit of the measured slope. All measurements were performed in air.

In between measurements, the samples were aged on a hotplate at either 150 °C or 180 °C in air in the dark, to estimate their stability. Initially, 150 °C was chosen to allow comparison with the literature (see below),[5] while at 180 °C, degradation proceeds sufficiently quickly to speed up the experiments. The results of the Seebeck coefficient S, the electrical conductivity σ, and the resulting power factor $S^2\sigma$ are shown in Figs. 3 and 4. Finally, samples were fully immersed in water for several minutes, to completely oxidize them and that way get an idea of a possible final state after long-term aging.

The electrical conductivity of all CNT salt samples is consistently higher than that of comparable films dispersed using SDBS, independently of the doping level. We attribute this to both the reduced bundle diameter seen in Fig. 2,[10,12] and the likely reduction in CNT length upon vigorous sonication.[24,25] Remarkably, this increase in σ is maintained even after completely oxidizing the films by immersing them in water, and thereby returning the doping level and Seebeck coefficient to that of regular air-exposed tubes. As a result, the power factor of the washed film is about five times higher than that of the SDBS-based samples.

Upon aging at elevated temperatures, we observe three different regimes, as indicated in Figs. 3 and 4. First, a relatively fast reduction in electrical conductivity accompanied by a small reduction in the absolute value of the Seebeck coefficient. Then, after about 50 h of aging, the response reaches a plateau, with little change up to about 600 h. Finally, for longer aging times, S quickly returns to its positive value. Similar behavior has been widely observed for both pristine[30] and doped CNT films,[7,31] and all of these superficially distinct regimes are commonly explained by the same process. Oxidation is due to atmospheric oxygen or water,[7,9,30–33] which initially proceeds quickly, and then slows down as the accessible active surface decreases.

Nonoguchi *et al.* were the first to report a thermoelectric material of this type, eDIPS CNTs doped with potassium hydroxide (KOH) and B18C6.[5] At 100 °C, they reported that S and σ are stable for at least 700 h, while at 150 °C S was stable for at least 600 h (at this temperature σ was not reported). They also mentioned that doping with just KOH was not successful, because the material could not effectively be turned n-type without the addition of crown ether.[5] In our case, even without any crown ether, we see a stability of the order of 500 h at 150 °C, and our results for σ and S of moderately aged samples closely agree with the values of Nonoguchi *et al.* reported for their samples aged at 100 °C, measured in the in-plane direction.[5]

We found, however, that the stability is strongly dependent on aging temperature. When it is increased to 180 °C, negative Seebeck coefficients persist only for about 30 h, as seen in Fig. 4. Reassuringly, addition of either 18C6 or B18C6 more than doubles the time before S returns to positive values. On the other hand, DB18C6 only slightly improves stability.

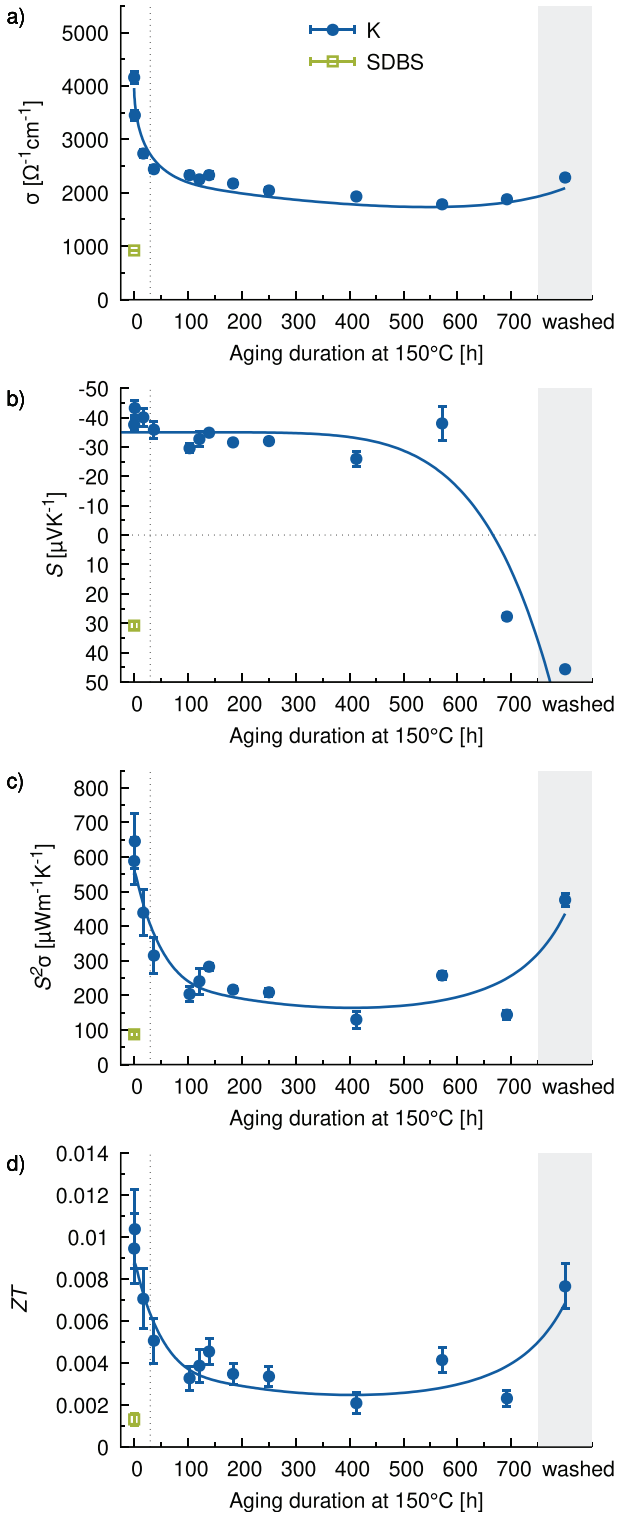

FIG. 3. TE performance of CNT salt aged at 150 °C, as well as of a reference buckypaper dispersed using SDBS. Lines are a guide to the eye.

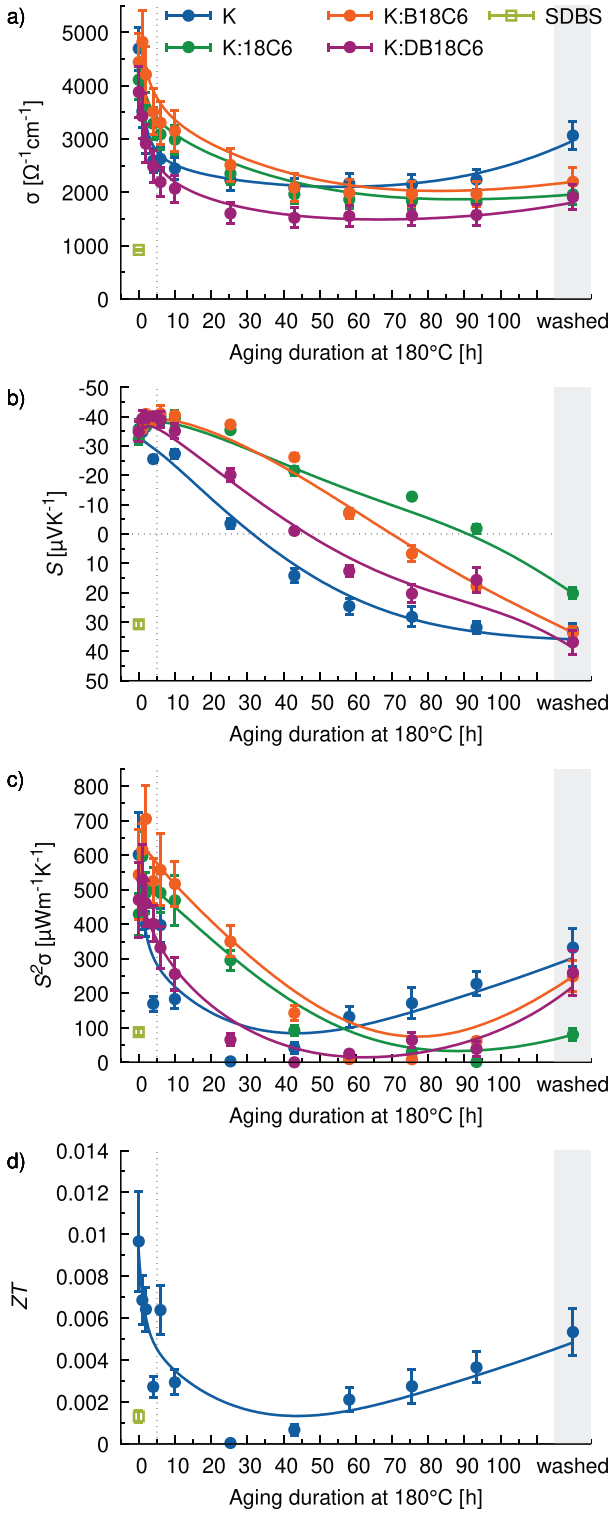

FIG. 4. TE performance of CNT salts without and with different crown ethers aged at 180 °C and of SDBS-dispersed reference buckypaper. Lines are a guide to the eye.

At this point, it should be mentioned that MacLeod *et al.* were not able to reproduce the stability of several n-type doping methods, including the one introduced by Nonoguchi *et al.*[6] They put forth several likely reasons, such as the lower diameter of the tubes used in their study, or the lack of metallic species in their polymer-sorted CNTs. However, another difference between the two studies that could explain the marked discrepancy in observed stability is the physical characteristics of the samples. Both Nonoguchi *et al.* and us used vacuum filtration to prepare buckypapers of considerable thickness (of the order of 10 to 100 μm, and $\approx$500 nm respectively), while MacLeod *et al.* used spray coating to deposit thin films of the order of 10 to 100 nm. These films not only differ in thickness, but potentially also in porosity, both of which may give rise to some form of self-encapsulation, potentially due to the accumulation of excess dopant. While this matter does warrant further investigation, it goes beyond the scope of the present work. Nonetheless, similar effects are not unheard of and were in fact reported for a dimethyl-dihydro-benzoimidazole (DMBI) based dopant, where it was shown that higher dopant coverage of CNTs (multilayer vs sub-monolayer) resulted in significantly improved stability.[31,34]

The in-plane thermal conductivity of free-standing samples was measured in high vacuum conditions (ca. 10^{-6} mbar) in a Linkam stage using One-Laser Raman Thermometry.[35] We employed the 488 nm line of an Ar^+ laser as excitation source in back-scattering geometry, together with a LabRam HR800 spectrometer (1800 grooves per mm) coupled to a liquid-nitrogen-cooled charge coupled device. For each of the samples, we first performed a temperature sweep to extract the corresponding Raman temperature shift coefficient of the characteristic *G*-peak of the nanotubes, located at about 1590 cm^{-1}.[36] Typical values were about $(-0.014 \pm 0.001)\,cm^{-1}\,K^{-1}$. This enabled us to quantify the temperature increase in the spot region as a function of the absorbed laser power, which was measured by assessing the incident, reflected and transmitted portions of the incoming beam. Typically, temperature resolution was about 3.5 K. For the deduction of the in-plane thermal conductivity, the corresponding two-dimensional heat equation for a free-standing film was solved and fitted to the experimental data in COMSOL Multiphysics. For this, we considered the film thickness as extracted from profilometry: an emissivity of 0.94 (as determined using an Optris PI 450 infrared camera); and a beam diameter of 2.2 $\pm$ 0.1 μm (as determined using the knife edge method with a 50$\times$ Olympus objective). Note that since the lateral dimensions of the free-standing portion are significantly larger than the beam spot size (mm^2 vs μm^2 respectively), we avoid border effects such as heat leakages with a hypothetical support, thus increasing the reliability of our experimental measurements.

Table I shows the results of the neat CNT salt, and of buckypaper prepared using SDBS, which agree well with previous reports.[37] The somewhat smaller thermal conductivity of the CNT salt might be

TABLE I. In-plane thermal conductivity κ of CNT films either dispersed by SDBS, or solubilized using potassium, without any crown-ether and before thermal aging.

Sample	κ ($W\,m^{-1}\,Km^{-1}$)
eDIPS:SDBS	27 $\pm$ 6
eDIPS:K	19 $\pm$ 3

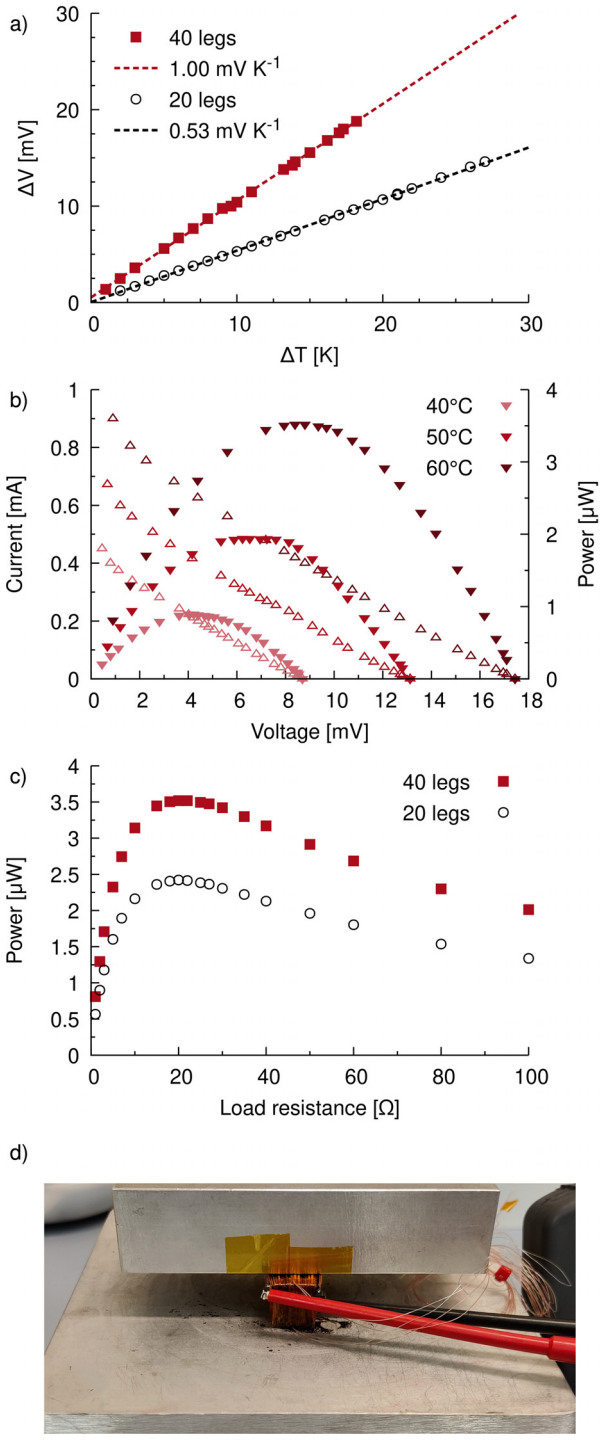

FIG. 5. Characterization of the modules. (a) Seebeck coefficients of the 40-leg (red) and 20-leg (black) module, obtained from a linear fit of ΔV vs ΔT. (b) Current and power of the 40-leg module vs voltage-drop across a variable load resistor at three different hot-side temperatures. (c) Power vs load resistance of both modules at a hot-side temperature of 60 °C. (d) Photo of the 40-leg module during characterization.

related to a change in porosity or bundle size. Figures 3(d) and 4(d) show the estimated thermoelectric figure of merit $ZT = \frac{S^2\sigma}{\kappa} T$ assuming that aging does not affect the thermal conductivity. We expect that the plotted values likely underestimate the real ZT, since when considering the Wiedemann–Franz law, one would expect that the observed reduction in electrical conductivity is accompanied by a corresponding reduction in the electronic contribution of the thermal conductivity.

As a final demonstration, we prepared modules with 20 and 40 legs, using B18C6 for the n-type legs, and SDBS for the p-type legs. The assembly process of the module is documented in Video 1 of the supplementary material, which shows a time lapse of the whole process.

Both modules have a nearly identical Seebeck coefficient of 26.5 and 25 μV K^{-1} leg^{-1} for the 20 and 40-leg version, respectively, as shown in Fig. 5(a).

This value is below the expected value of 30 to 40 μV K^{-1} leg^{-1}. To understand these results, some of the films from the same batch as those used for the module were characterized separately, and their Seebeck coefficients were measured. The values obtained were 30.8 ± 1.4 μV K^{-1} for the p-type SDBS legs, and -34.1 ± 3.1 μV K^{-1} for the n-type B18C6 legs. The differences between per-module and per-leg characterization are likely due to geometric effects and imperfections in the module manufacturing process. As can be seen in Video 1, the silver paste contacts are not identical for all legs. Similarly, the hot and cold sides are not flat surfaces, but instead, neighboring legs are somewhat offset in height from each other. Because of this, the actually applied temperature gradient across the module may be less than the measured difference at the hot and cold side, resulting in less than optimal performance.

We characterized both modules by placing them on a hotplate at 40 °C, 50 °C, and 60 °C and weighing them down with an aluminum block that served as a heat sink, as pictured in Fig. 5(d). After 30 min, we measured stable temperature differences of 13.4, 19.6, 25.7 K and 8.4, 12.6, 17.2 K for the 20- and 40-leg module, respectively. Results of the 40-leg module are plotted in Fig. 5(b). As expected, the generated power scales with the square of ΔT. Fig. 5(c) directly compares both modules with each other. While the 40-leg module generates more power (3.5 vs 2.4 μW), the 20-leg module is not far behind, since it can sustain a significantly higher ΔT. Both modules have an internal resistance of approximately 21 Ω, since the relative active films thickness of the 40-leg module was chosen to be double that of the 20-leg module.

In summary, we have investigated the thermoelectric properties and stability of CNT salts. We presented a method that allows to prepare films of n-doped CNTs with reduced bundle size, and without having to resort to damaging sonication, which is known to shorten tubes. The films are stable over hundreds of hours at 150 °C, and even after being completely dedoped, their thermoelectric performance is superior to that of films prepared using sonication and surfactants.

See the supplementary material for a time lapse video of the assembly process of the module.

The authors acknowledge financial support from the Spanish Ministry of Science and Innovation through the "Severo Ochoa" Program for Centers of Excellence in R&D (No. CEX2019-000917-S), Nos. PGC2018-095411-B-I00 and MAT2017-90024-P

(TANGENTS)-EI/FEDER; from the Generalitat de Catalunya and European Union (FEDER) through AGAUR 2018 PROD 00191; and from the European Research Council (ERC) under Grant Agreement No. 648901. We also thank Professor Alejandro R. Goñi (ICMAB) for fruitful discussions.

DATA AVAILABILITY

The data that support the findings of this study are available from the corresponding author upon reasonable request.

REFERENCES

[1]J. L. Blackburn, A. J. Ferguson, C. Cho, and J. C. Grunlan, Adv. Mater. **30**, 1704386 (2018).
[2]A. D. Avery, B. H. Zhou, J. Lee, E.-S. Lee, E. M. Miller, R. Ihly, D. Wesenberg, K. S. Mistry, S. L. Guillot, B. L. Zink, Y.-H. Kim, J. L. Blackburn, and A. J. Ferguson, Nat. Energy **1**, 16033 (2016).
[3]K. Yanagi, S. Kanda, Y. Oshima, Y. Kitamura, H. Kawai, T. Yamamoto, T. Takenobu, Y. Nakai, and Y. Maniwa, Nano Lett. **14**, 6437 (2014).
[4]G. Zuo, Z. Li, E. Wang, and M. Kemerink, Adv. Electron. Mater. **4**, 1700501 (2018).
[5]Y. Nonoguchi, M. Nakano, T. Murayama, H. Hagino, S. Hama, K. Miyazaki, R. Matsubara, M. Nakamura, and T. Kawai, Adv. Funct. Mater. **26**, 3021 (2016).
[6]B. A. MacLeod, N. J. Stanton, I. E. Gould, D. Wesenberg, R. Ihly, Z. R. Owczarczyk, K. E. Hurst, C. S. Fewox, C. N. Folmar, K. Holman Hughes, B. L. Zink, J. L. Blackburn, and A. J. Ferguson, Energy Environ. Sci. **10**, 2168 (2017).
[7]M. Shim, A. Javey, N. W. Shi Kam, and H. Dai, J. Am. Chem. Soc. **123**, 11512 (2001).
[8]C. Cho, N. Bittner, W. Choi, J.-H. Hsu, C. Yu, and J. C. Grunlan, Adv. Electron. Mater. **5**, 1800465 (2019).
[9]F. Abdallah, L. Ciammaruchi, A. Jiménez–Arguijo, E.-S. M. Duraia, H. S. Ragab, B. Dörling, and M. Campoy–Quiles, Adv. Mater. Technol. **5**, 2000256 (2020).
[10]P. E. Lyons, S. De, F. Blighe, V. Nicolosi, L. F. C. Pereira, M. S. Ferreira, and J. N. Coleman, J. Appl. Phys. **104**, 044302 (2008).
[11]P. N. Nirmalraj, P. E. Lyons, S. De, J. N. Coleman, and J. J. Boland, Nano Lett. **9**, 3890 (2009).
[12]K. Mustonen, P. Laiho, A. Kaskela, T. Susi, A. G. Nasibulin, and E. I. Kauppinen, Appl. Phys. Lett. **107**, 143113 (2015).
[13]B. Norton-Baker, R. Ihly, I. E. Gould, A. D. Avery, Z. R. Owczarczyk, A. J. Ferguson, and J. L. Blackburn, ACS Energy Lett. **1**, 1212 (2016).
[14]Q. W. Li, Y. Li, X. F. Zhang, S. B. Chikkannanavar, Y. H. Zhao, A. M. Dangelewicz, L. X. Zheng, S. K. Doorn, Q. X. Jia, D. E. Peterson, P. N. Arendt, and Y. T. Zhu, Adv. Mater. **19**, 3358 (2007).
[15]A. Pénicaud, P. Poulin, A. Derré, E. Anglaret, and P. Petit, J. Am. Chem. Soc. **127**, 8 (2005).
[16]D. Voiry, C. Drummond, and A. Pénicaud, Soft Matter **7**, 7998 (2011).
[17]A. Pénicaud, F. Dragin, G. Pécastaings, M. He, and E. Anglaret, Carbon **67**, 360 (2014).
[18]C. Jiang, A. Saha, C. Xiang, C. C. Young, J. M. Tour, M. Pasquali, and A. A. Martí, ACS Nano **7**, 4503 (2013).
[19]C. Jiang, A. Saha, C. C. Young, D. P. Hashim, C. E. Ramirez, P. M. Ajayan, M. Pasquali, and A. A. Martí, ACS Nano **8**, 9107 (2014).
[20]C. Jiang, A. Saha, and A. A. Martí, Nanoscale **7**, 15037 (2015).
[21]D. Voiry, O. Roubeau, and A. Pénicaud, J. Mater. Chem. **20**, 4385 (2010).
[22]Y. Y. Huang, T. P. J. Knowles, and E. M. Terentjev, Adv. Mater. **21**, 3945 (2009). arXiv:0907.3176.
[23]A. Lucas, C. Zakri, M. Maugey, M. Pasquali, P. van der Schoot, and P. Poulin, J. Phys. Chem. C **113**, 20599 (2009).
[24]A. Graf, Y. Zakharko, S. P. Schießl, C. Backes, M. Pfohl, B. S. Flavel, and J. Zaumseil, Carbon **105**, 593 (2016).
[25]A. J. Clancy, D. B. Anthony, S. J. Fisher, H. S. Leese, C. S. Roberts, and M. S. P. Shaffer, Nanoscale **9**, 8764 (2017).
[26]D. D. Tune, A. J. Blanch, C. J. Shearer, K. E. Moore, M. Pfohl, J. G. Shapter, and B. S. Flavel, ACS Appl. Mater. Interfaces **7**, 25857 (2015).
[27]B. Dörling, O. Zapata-Arteaga, and M. Campoy-Quiles, Rev. Sci. Instrum. **91**, 105111 (2020).
[28]X. He, J. Yang, Q. Jiang, Y. Luo, D. Zhang, Z. Zhou, Y. Ren, X. Li, J. Xin, and J. Hou, Rev. Sci. Instrum. **87**, 124901 (2016).
[29]L. J. van der Pauw, Philips Tech. Rev. **20**, 220 (1958).
[30]P. G. Collins, K. Bradley, M. Ishigami, and A. Zettl, Science **287**, 1801 (2000).
[31]Y. Nakashima, R. Yamaguchi, F. Toshimitsu, M. Matsumoto, A. Borah, A. Staykov, M. S. Islam, S. Hayami, and T. Fujigaya, ACS Appl. Nano Mater. **2**, 4703 (2019).
[32]X. Peng, Z. Liu, J. Yao, H. Li, Y. Zhang, G. Yan, and F. Du, Synth. Met. **266**, 116429 (2020).
[33]Y. Iihara, T. Kawai, and Y. Nonoguchi, Chemistry **15**, 590 (2020).
[34]Y. Nakashima, N. Nakashima, and T. Fujigaya, Synth. Met. **225**, 76 (2017).
[35]A. A. Balandin, S. Ghosh, W. Bao, I. Calizo, D. Teweldebrhan, F. Miao, and C. N. Lau, Nano Lett. **8**, 902 (2008).
[36]M. Dresselhaus, G. Dresselhaus, R. Saito, and A. Jorio, Phys. Rep. **409**, 47 (2005).
[37]D. Abol-Fotouh, B. Dörling, O. Zapata-Arteaga, X. Rodríguez-Martínez, A. Gómez, J. S. Reparaz, A. Laromaine, A. Roig, and M. Campoy-Quiles, Energy Environ. Sci. **12**, 716 (2019).